

Radiation Detection and Situation Management by Distributed Sensor Networks

Janette Frigo^a, Sean Brennan^a, Ernst Esch^a, Diana Jackson^a, Vinod Kulathumani^b, Edward Rosten^c,
Patrick Majerus^a, Adam Warniment^a, Angela Mielke^a, and Michael Cai^a

^aLos Alamos National Laboratory, P.O. Box 1663, MS D440, Los Alamos, NM 87545;

^bDepartment of Computer Science and Electrical Engineering, West Virginia University, P.O. Box 6109, Morgantown, WV, 26506-6109;

^cDepartment of Engineering, Cambridge University, Cambridge, CB3 0SD, England

ABSTRACT

Detection of radioactive materials in an urban environment usually requires large, portal-monitor-style radiation detectors. However, this may not be a practical solution in many transport scenarios. Alternatively, a distributed sensor network (DSN) could complement portal-style detection of radiological materials through the implementation of arrays of low cost, small heterogeneous sensors with the ability to detect the presence of radioactive materials in a moving vehicle over a specific region. In this paper, we report on the use of a heterogeneous, wireless, distributed sensor network for traffic monitoring in a field demonstration. Through wireless communications, the energy spectra from different radiation detectors are combined to improve the detection confidence. In addition, the DSN exploits other sensor technologies and algorithms to provide additional information about the vehicle, such as its speed, location, class (e.g. car, truck), and license plate number. The sensors are in-situ and data is processed in real-time at each node. Relevant information from each node is sent to a base station computer which is used to assess the movement of radioactive materials.

Keywords: distributed sensor networks, radiation detection, heterogeneous sensors

1. INTRODUCTION

Many vehicle surveillance radiation detection applications utilize portal monitor-style radiation detectors. These detectors are extremely accurate, but are large and costly. Additionally portal monitors require the use of traffic choke points to ensure vehicles pass through the portals at slow speeds and in a single-file configuration. This approach is viable in applications where a limited number of traffic routes are to be monitored in high value areas where significant sensor cost is tolerable. In such applications personnel are readily available to investigate potential alarms immediately, thus ensuring false alarms are quickly mitigated.

In contrast there are a host of applications in remote areas where choke points do not exist and personnel are not readily available. In these instances small, dispersed, autonomous and cost effective sensor systems are needed to provide a warning of potential threats, particularly for rapid deployment. These systems, though, need to maintain extremely small false alarm rates, a task that is extremely difficult given the requirement for small, low power, radiation detection technology.

Research is ongoing at LANL developing networks of heterogeneous, low cost sensors. This approach ensures data from several types of sensors are combined to provide highly confident decisions as to the presence and type of vehicles in remote, monitored regions and the presence of radiological material. Such networks process raw data at the sensor and propagate the multi-modal information over the network, allowing timely decisions to be made remotely by monitoring personnel. Instead of relying solely on a single large radiation detector, decisions are made based on a combination of corroborating evidence from multiple sensors. In our field experiments the monitoring network employed seismic sensors to detect the presence of a vehicle, acoustic sensors to determine the type of vehicle, photo sensors to collect license plate information about the monitored vehicle and radiation detectors to determine the presence

of radioactive materials. Such a system has been successfully demonstrated in remote canyons within the LANL complex and has the ability to significantly alter the methods currently utilized to provide wide area persistent surveillance.

The remainder of this paper is organized as follows: Section 2 describes our approach for detection of radiological materials in moving vehicles and how it compares to that of the research community. Section 3 discusses the heterogeneous sensors nodes; the algorithms and the deployed system implementation. Section 4 explains our field experiment; the communication system, base station graphical user interface (GUI), and field test setup. Finally, in Section 5 we show our system test results for the DSN.

2. RELATED WORK

Simulation test beds are an important first step in any sensor network system. However, moving from the simulation test bed to hardware implementation is costly and time consuming for any deployed system whether the system is a satellite; a mobile robot or a sensor network. Most sensor network research for radiation detection is in simulation only, such as in Parunak's [2] simulation for radiation detection and situational management, a large dynamic spatio-temporal configuration of sensors are used. Others discuss the challenges and possible solutions of transportation security, including intra-modal transport venues, using knowledge discovery tools [1].

In our own previous work, the Distributed Sensor Network project at LANL looked at the feasibility of a small network of sensor nodes using PDA-sized platforms for processing raw gamma counts [3]. In [4] and [5] the feasibility of a network of detectors for measuring radioactive materials along a known trajectory and the ramifications thereof are examined. In [6] the effectiveness of scaling large numbers of nodes (greater than 10) and changing source trajectory parameters versus the computational demands required for such a task are explored.

In this paper we report our attempt to implement a deployed multi-modal sensor network for the detection of moving radioactive materials along a roadway. The goal of this work reported herein is to implement the system using low power, Commercial Off-The-Shelf (COTS) hardware and thereby evaluate its effectiveness. Our approach is to use low power, wireless sensor nodes. For detection of radioactive material, multiple radiation detectors sum spectra using coherent addition to obtain an increase in signal-to-noise compared to a single detector, thus, by increasing the number of detectors, the *collected* spectrum is significantly improved.

3. HETEROGENEOUS SENSOR NODES

This section describes the system configuration, algorithms, and implementation for the three types of sensor nodes in our DSN system: vehicle class identification, vehicle license plate detection, and radiation detection.

3.1 Vehicle Class Identification

The goal of this vehicle classifier node is to classify vehicles as they traverse a region of influence into one of three categories: a small compact car, a moderately heavy vehicle and a very heavy vehicle. For our training and testing we chose a 1994 Honda Accord LX, manual drive compact car, a 2006 Diesel Chevy C4500 4x4 truck, and a 1994 HumV H-1 with a 6.5 L Detroit Diesel Engine as representative vehicles of each category. We assume that vehicles do not enter the monitoring area concurrently. Particular challenges and assumptions for this classifier node are: (1) Vehicles travel between 10 to 40 mph and stay within the influence region of the sensors for a very short time of 1 to 2 seconds only; (2) The audio spectral signature of the vehicle can change over time; (3) The algorithms cannot be computationally intensive.

Vehicle classifier implementation

The vehicle classifier node developed uses seismic and acoustic sensors connected to a Crossbow Mica2 mote and a Stargate respectively (see Figure 1). The seismic sensor is a GeoSpace geophone placed 50 feet from the road to eliminate acoustic feedback in the sensor. The geophone is connected to the Mica2 via a custom signal conditioning interface board and a 16-bit A/D board. The acoustic sensor is a Samson C01U USB Studio Condenser Microphone, placed 10-12 feet from the road and mounted 1 foot off the ground. The microphone is connected directly via a USB port to the Stargate (400 MHz, Intel PXA255 Processor, Linux based). The microphone has directional response and is mounted facing toward the roadway. Windshields on the microphones help filter wind noise.



Figure 1 Mica2 mote, signal conditioning box, seismic sensor (left). Stargate and acoustic sensor (right)

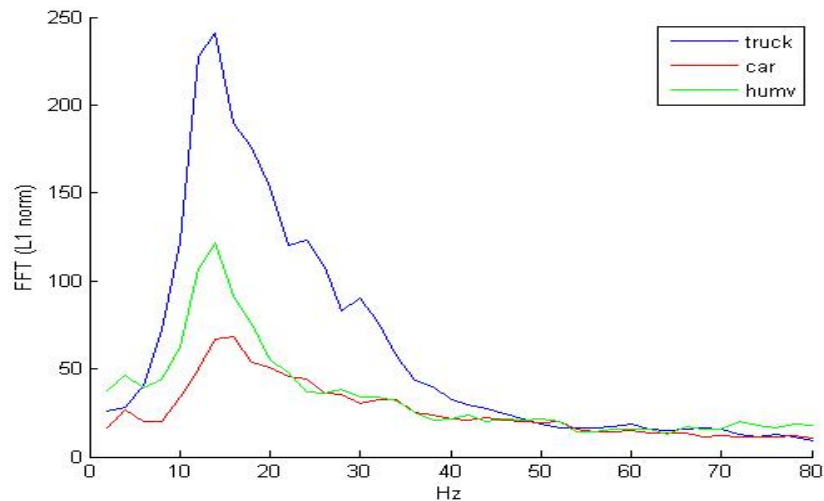


Figure 2 Frequency characteristics of seismic detection

This implementation uses the Mica2 mote to trigger an *event* based on seismic information. The event is transmitted to the Stargate processor over the 900 MHz radio link. The Stargate then samples the microphone and processes acoustic information and sends a stream of classifications to a base station computer (via an 802.11 network). We use this method of seismic detection triggered acoustic sampling and processing because it is an energy efficient way of fusing the multi-sensor information to yield a single classification, i.e. the seismic detection runs continuously at approximately 60 milliWatts compared to the Stargate/acoustic processing which takes about 2.4 Watts. Moreover, the frequency characteristics for seismic detection show very similar peak frequencies (see Figure 2) so more frequency analysis would

have to be done in order to develop an accurate classification using only seismic data and the Mica2 does not have sufficient computing capabilities to do this. For these reasons, we choose to combine both seismic and acoustic sensors to achieve a more reliable, energy-efficient classification.

Vehicle classifier algorithms

The geophone is sampled at 100 Hz. The Mica2 mote computes the Haar Wavelet on a moving window. The Haar wavelet is computed up to level 2 which computes the energy estimate of the 12-24 Hz band via the average of the coefficients of this band. The variance of the energy estimate is computed (see Figure 3). A variance threshold is used for vehicle *event* detection. A trigger is sent to the Stargate over the radio link when a vehicle event occurs. The Haar Wavelet is chosen for its low-level of computational complexity, a requirement due to the 8-bit computing capability of the ATMEL processor on the Mica2 [7] and also because of the narrow peak frequency observed for all the vehicle categories.

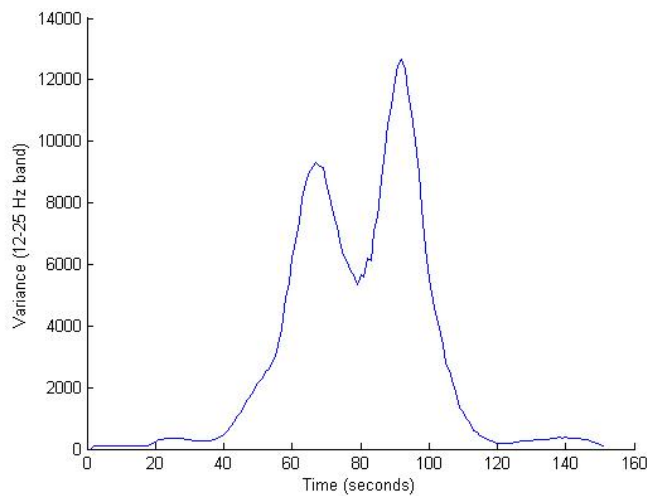


Figure 3 Moving window variance characteristics of 12- 25 Hz band for a 'truck' class

Upon receiving a trigger, the microphone is sampled at 4 kHz. There are four sources of sound collected by the acoustic sensor, i.e. road/tire, engine, mechanical and air current noise. For the classifier, a 512-point integer FFT is implemented on the Stargate. The 512-point FFT is computed to obtain the spectral characteristics of the data, yielding an 8 Hz resolution. Frequencies lower than 64 Hz are not used due to variations in the microphone response and temporal variations (wind) at these lower frequencies.

We first obtain training data sets using multiple runs of each vehicle at different speeds. We use the samples collected during the 2 seconds when the vehicle is closest to the microphone for the training. We then identify the ideal feature vector set to do the classification between each pair of vehicles. For example to classify between a car and a truck, we use a 10 coefficient vector, formed by the average energy of 10 equally spaced bands in the 224 Hz to 368 Hz range because the spectral characteristics of the truck shows a distinctive spike in response at those frequencies. We use Fisher Linear Discriminant Vector analysis to identify the best projection vector given the training data. We obtain a similar projection vector to distinguish whether the vehicle is a Humv or a car/truck. These projection vectors are computed offline in matlab and then copied into the classifier program running on the Stargate.

In every round, the Stargate simply computes the dot product of this vector with the feature vector obtained in that round to perform the classification. The Stargate first classifies whether the vehicle is a Humv or either of car or truck. Then it classifies whether the vehicles is a car or a truck. We find that this is the classification order that maximizes the distance between classes.

Once triggered the classifier operates for a few seconds as the vehicle passes the sensor. The acoustic classifier is operating in real-time and generates a classification output once every 125 ms. The characteristics of an approaching

vehicle differ from when the vehicle is at the closest distance to the sensor. The base station computer integrates the individual classification outputs to generate the final classifier output.

Vehicle classifier accuracy

We achieved no false negatives from the seismic sensor during 10 field trials. A person walking as close as 2 feet away from the sensor does not trigger an event. A person jumping less than 10 feet away from the sensor triggers a seismic detection; however this case can be isolated using temporal characteristics.

The initial work on the acoustic classifier also showed zero misclassification's in 10 test runs of each vehicle class. Note that, we maintain our testing environment to be similar to the training environment. We also ensure that vehicles enter the field one at a time. Training the classifier in a dynamic manner to different environments is a much more difficult problem and is a subject of future work.

3.2 License Plate Detection

The vehicle license plate detection node aims to capture the image of a vehicle traveling on the roadway, reduce the image to license plate pixels only using a learning algorithm and resize this reduced image for efficient transfer over the network to the base station. The image processing algorithm reduces the original image by 60 to 90%, and allows the image to be converted to text via an Optical Character Recognition (OCR) application on the base station.

License plate node implementation

The video sensor node consists of a webcam (with a 12 mm telephoto lens) and a magnetometer (HMR2300-232) connected directly to the Stargate via the USB port and the serial port respectively. The magnetometer is used as a trigger for image capture. A learning algorithm converts the original image to license plate pixels only. This processed image information is sent over the 2 GHz wireless link to the network. The sensors and Stargate are mounted approximately 10 feet away from the road and 3 to 4 feet off the ground. To eliminate glare, the assembly is slanted at about a 45 degree angle to the road.

The system requirements are as follows: to capture a 640x480 pixel image of the aft end of a vehicle at anticipated vehicle speeds of 10 to 60 mph, to extract the license plate pixels only from the original image, thereby reducing the original image by approximately 60-90%.

Figure 4 shows a vehicle image captured from the webcam. We use the webcam due to its ease of integration, low power, low cost and compact size. In addition, the image resolution with our telephoto lens was sufficient for the learning algorithm. The best range for image capture is within 8 to 15 feet from the camera. The magnetometer triggers on the front end of the vehicle and we capture images for 5 seconds at approximately 10 frames/sec. From this set of frames, one original image is chosen to be processed.



Figure 4 License plate image capture

License plate detection algorithms

The processing on the license plate detection node works by applying a classifier to every pixel in an image to create a rough segmentation of the license plate, if it exists. From this, the bounding box of the license plate is found, and that section of the image is then resampled to a fixed size. The resampled image is then compressed and sent over the

network. These steps are a trade off between the amount of network bandwidth used, the latency of the operation and the amount of computing power used locally.

The classifier is trained using data collected during typical field operation. This consists of various vehicles viewed at distances of between 8 and 75 feet from the camera, as well as some 'background' images containing no license plates. Eight bpp greyscale images are used for the algorithm development.

The license plate detection software has to be able to process full video images on the Stargate processor, so a very efficient algorithm is required. The license plate detection is performed using a machine learning algorithm, trained on labeled data. To achieve very high speed video processing we use an algorithm which takes elements from two algorithms known to produce very efficient classifiers, namely the Viola-Jones [8] object detection algorithm and the ID3 [9] decision tree classifier. The algorithm details for license plate segmentation, bounding and resampling are found in [10]. Figure 5 shows a sample output from the license plate detection node.

Accuracy determination for the license plate detection node, and conversion of license plate images to text are topics of future research.



Figure 5 License plate detection output image

3.3 Radiation Detection

Whereas our other sensing nodes could operate in a rather loosely-coupled fashion to arrive at conclusions, our radiation detection nodes were much more tightly coupled. Our hypothesis – that multiple small detectors working in concert can be substituted for one large detector – in fact requires this strong cooperation. We equipped two Stargate nodes with Amptek GAMMA-RAD 76 x 76 mm (3") NaI scintillators, and a third with an Amptek GAMMA_RAD 10 x 10 x 40 cm (4" x 4" x 16") NaI detector. These three nodes collected background and triggered-signal data and transmitted that data wirelessly to a fourth node which combined and processed all this data into a single spectrum for examination. For background calibration purposes a small bag of potassium-chloride was placed next to the detectors.

Radiation detection implementation

To distinguish when a vehicle occupies the space in front of the radiation detector, we use a magnetometer to trigger the node. Each node is setup to take data in the form of a ring buffer filled with radiation spectra. Each spectrum displays the gamma-ray energies present for a certain amount of time t . In this case the time is three seconds. By generating a ring buffer with n spectra, it is possible to access the radiation response for a time $t*n$ in the past after the trigger occurred. Once a trigger occurs, the node collects a predetermined number of spectra as radiation signal. In our experiment three spectra were taken. A background, extracted from the circular buffer at the previous time (21 seconds), is computed by summing a certain amount of background spectra. To keep subtraction errors low, the background sum is composed of 50 spectra and then scaled to the radiation spectra time. The two resulting spectra, radiation signal and background, are sent to a radiation processing node. The signal spectra are deleted from the ring buffer and thereby the detector is ready for a new trigger.

At the radiation processing node the data is received and the difference between the radiation source spectrum and the background spectrum is calculated. The background spectra from each sensor are separately analyzed for the position of the potassium-chloride peak at 1461 keV. The resulting data calibration point is used for energy calibration each time a trigger occurs. This algorithm is necessary to prevent energy calibration drift in sodium-iodide detectors (see Figure 6)

[11]. Our target radioisotope is Cesium-137 (^{137}Cs) with an activity of 300 microcuries. It is mounted on the near side of the bed of a Chevy 4x4 truck.

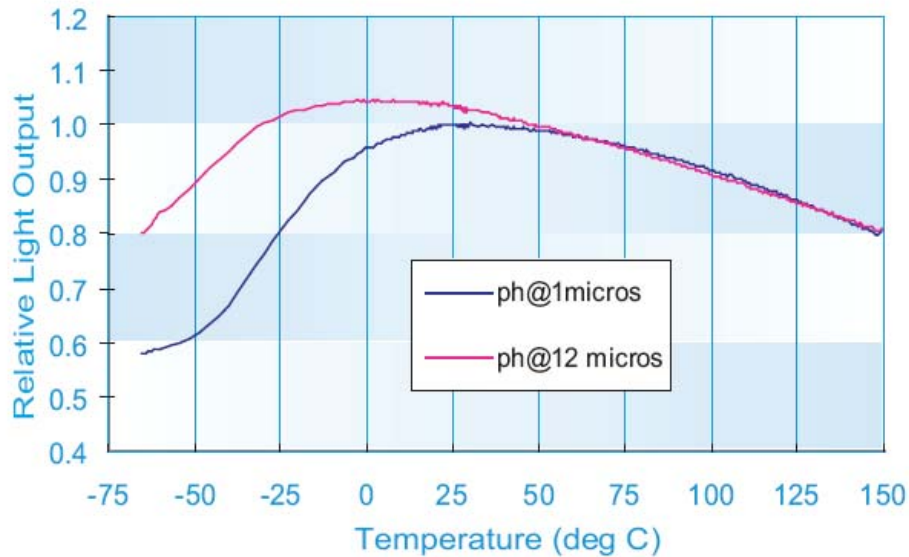


Figure 6 Nai Temperature dependant light output for NaI(Tl) chrystals [11].

Once the data calibration is completed for each of the three spectra, each spectrum is filled into a new spectrum with a 1keV bin width. The filling process is done by an algorithm that calculated the overlap of the old spectrum bin with the new spectrum bin. The old bin value is multiplied by an overlap to bin-width ratio and filled into the new bin. Once this process is completed, the spectra from the different NaI(Tl) detectors are added into a sum-spectrum. This sum-spectrum now displays the radiation coming from the suspect vehicle added over 3 detectors.

4. FIELD EXPERIMENT

In this section, we describe the overall DSN system layout for our field experiment including the sensor and base station nodes, the network communication, and our test scenarios.

4.1 Network communication

We use direct 802.11 connections from each node to the base station computer. Initially, our first attempt used several multi-hop nodes between the sensors and the base station. However, due to the hot outdoor temperatures our 802.11 cards failed intermittently. As well, issues arose with our custom message passing/routing software and it was decided to implement a direct 802.11 connection between the sensor nodes and the base station. We used TCP/IP connections for their robustness.

Base Station GUI

The DSN GUI was developed in Java to provide a visual representation of the status of the sensor nodes within the DSN network. The GUI operates in one of two modes: playback and real-time. In real-time mode, the GUI receives data packets from the radiation processing node, three vehicle classifier nodes, and the video node. Each vehicle classifier node sends a stream of classifications as the vehicle approaches and passes the seismic/acoustic sensors. An algorithm for vehicle identification processes this stream of data and determines a vehicle *class* for each node. (This final step could be implemented on the individual nodes, but for debugging and testing purposes it is done at the base station computer.) Then a confidence level out of the possible number of nodes is displayed. The license plate detection node

sends a compressed png image of license plate pixels only. Currently, this license plate image is displayed along with the vehicle classification and confidence level per Figure 7. The final step to convert the license plate pixels to text using an OCR application is forthcoming. The intention is to be able to check a data-base of allowable license plate numbers and the time and date to verify traffic activity. For the three radiation nodes, a fourth *radiation processing node* receives the spectra from each radiation sensor node and computes the combined background spectra, the detected source spectra (signal minus background) and sigma level. The GUI displays the *spectral data* graph (detected source spectra) for the radiological material (^{137}Cs) in counts and the *subtractive background data* information (see Figure 7). Finally, for vehicle tracking the GPS location of each node and the system clock is used to derive vehicle speed and location.

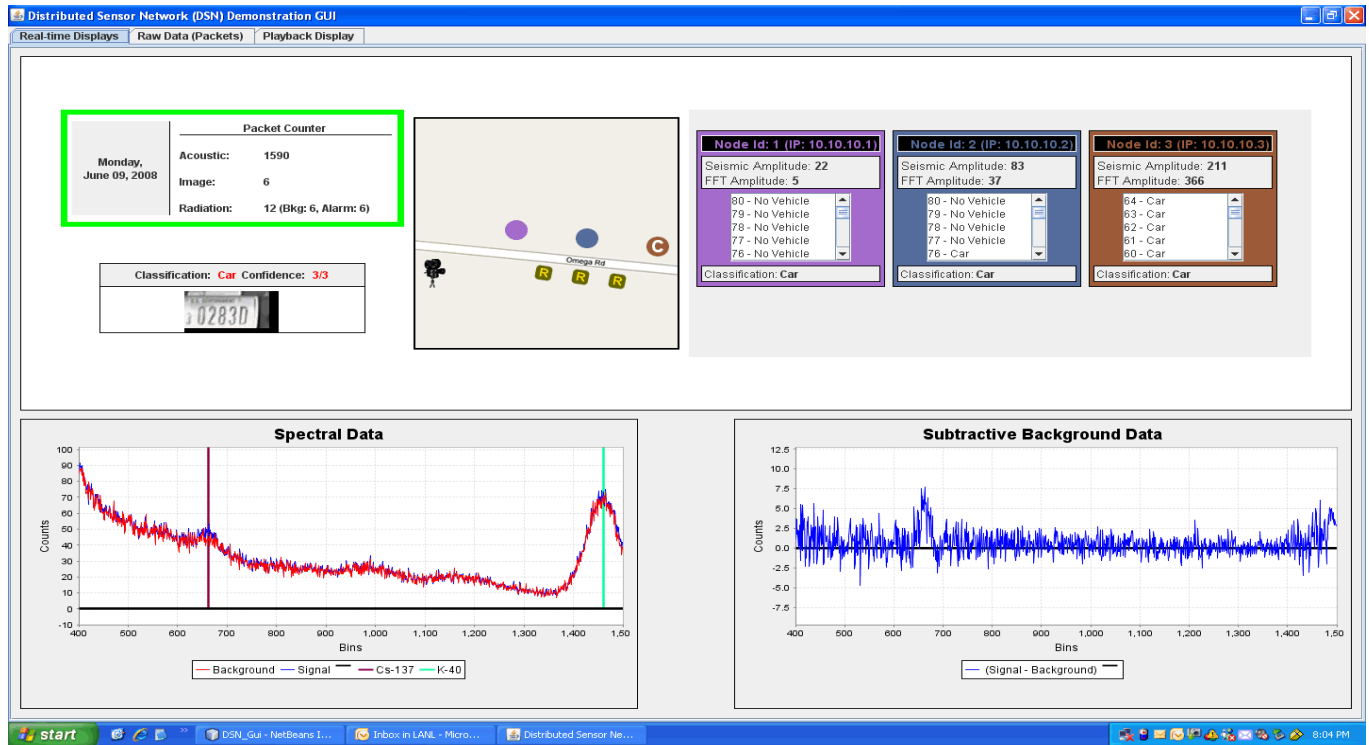


Figure 7 DSN field experiment GUI

The base station GUI is essential for situational management as it allows monitoring personnel to get an immediate analysis of the spectral data in comparison with the background data to help determine the presence of a radioactive material. In addition, it provided a real-time display of sensor nodes to determine vehicle class, license plate, and vehicle speed and location (not displayed in Figure 7) to aid in verifying normal and suspicious traffic movement.

4.2 Test System Configuration

Figure 8 shows the DSN system layout for our field experiment. Our field demonstration included seven sensor nodes; three vehicle classification nodes, three radiation detection nodes (and a fourth radiation processing node), and one license plate detection node. Sensor nodes are placed approximately 125 feet apart. The three radiation nodes communicate to the radiation processing node and it communicates directly via an 802.11 wireless link to the base station. All other sensor nodes communicate directly to the base station computer. The total distance covered on the roadway for this experiment is approximately 625 feet from end-to-end.

The test scenario consisted of multiple test trials per vehicle (car, truck, and HumV) traveling east bound on the roadway with varying speed of 5, 10, 25, and 40 mph. A five minute *rest* interval between trials existed so we could check system readiness. The vehicle containing the radioactive materials, a Chevy 4x4 truck, was tested at speeds of 5 to 10 mph with multiple trials.

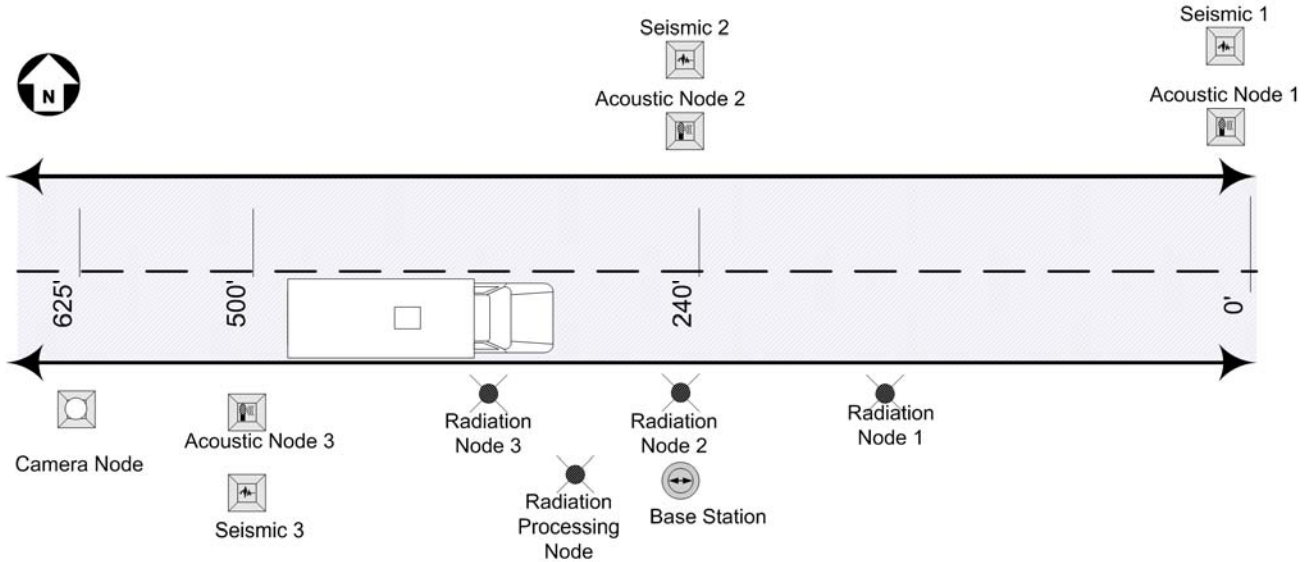


Figure 8 DSN test demonstration configuration

5. RESULTS

5.1 Vehicle Identification

The vehicle classifier nodes performed nominally for the compact car and HumV trials at speeds of 10, 25, 40 mph, each classified 100%. The vehicle containing the radioactive materials, a Chevy 4x4 truck, drove at speeds of 5 and 10 mph and was classified as a *car* with a confidence of 100 % (see Figure 7) since this vehicle has similar frequency characteristics to the compact car at these slow speeds. For the license plate detection node the HumV and the car did not classify correctly on three trials because it was not part of the training data for the learning algorithm and the license plate is located on the bottom left of the vehicle--the algorithm (in Section 3.2) is searching for the license plate pixels in the center of the frame between the 25th and 70th percentile horizontally and vertically. This problem can be addressed with an improved vehicle image data set for algorithm development and further refinement of the learning algorithm. For the car, the license plate detection was not accurate over three trails due to glare from the sun because the direction of travel was east bound in mid morning. This problem can be easily mitigated with a protective shield for the camera.

5.2 Radiation detection

Figures 9 and 10 are the combined background spectrum overlapping the combined signal spectrum and the difference between the two, respectively, for a non-isotope pass. Note the drastic change in the Y-axis values between these two figures. Figures 11 and 12 correspond to the Cesium pass. The photopeaks for ^{40}K and ^{137}Cs are marked. The Y-axes for Figures 9 and 11 and for Figures 10 and 12 are identical for clarity of comparison. Vehicles passing without a radioactive source have no peak at 662 keV corresponding to ^{137}Cs as is just visible in Figure 11 but more obvious in Figure 12. Also note the increased counts overall for the radioisotope pass. Our calibration was somewhat imperfect in scaling, hence the peak in Figure 12 at 1461 keV (^{40}K), but the Cesium peak is very distinct.

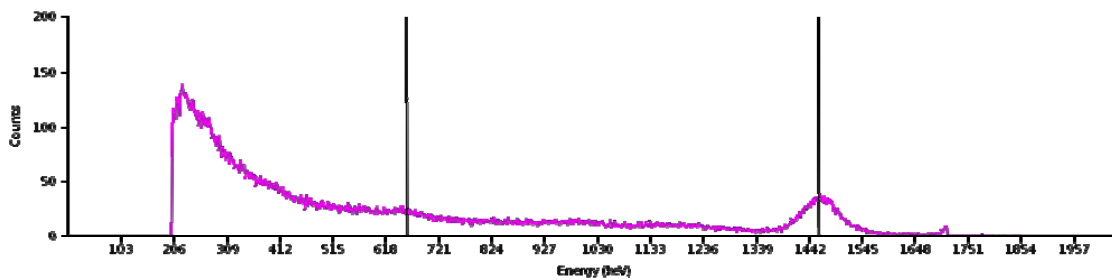


Figure 9 Signal and background spectra for a vehicle without radioactive material.

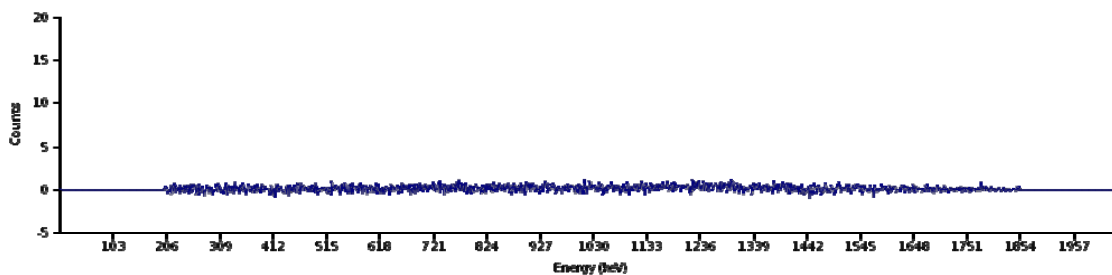


Figure 10 Difference between signal and background spectra for a vehicle without radioactive material.

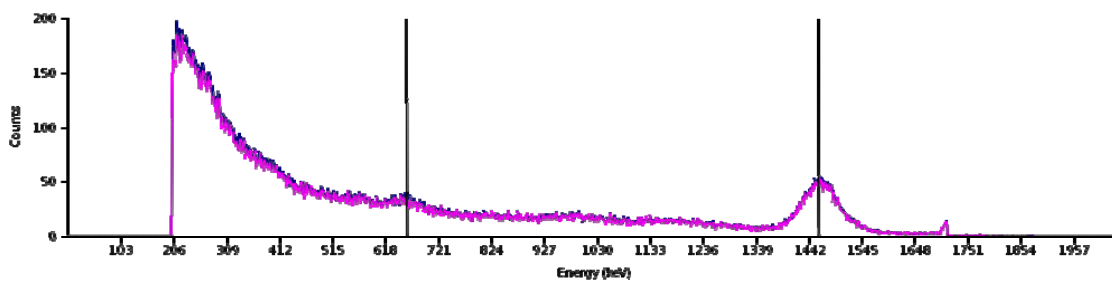


Figure 11 Signal and background spectra for a vehicle carrying ^{137}Cs

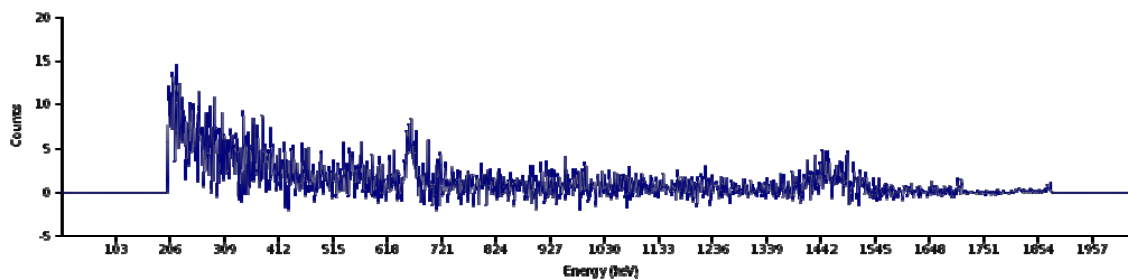


Figure 12 Difference between signal and background spectra for a vehicle carrying ^{137}Cs

6. SUMMARY

A distributed sensor network may complement portal-style detection of radiological materials through the implementation of arrays of low cost, small heterogeneous sensors with the ability to detect the presence of radioactive materials in a moving vehicle over a specific region. In this paper, we report on the use of a heterogeneous wireless sensor network for traffic monitoring in a field demonstration setting. Through wireless communications, the energy spectra from different radiation detectors are combined to improve the detection confidence. In addition, the DSN exploits other sensor technologies and algorithms to provide information about the vehicle, such as its speed, location, class (e.g. car, truck), and license plate number. Multi-modal DSNs are a potential radiation detection capability, enabling deployment over a broader region without the loss of detection accuracy.

ACKNOWLEDGEMENTS

This work was supported by the U. S. Department of Energy/NNSA and Los Alamos National Laboratory funds under LANS, LLC Contract No. W-7405-ENG-36. This document is approved for public release under LAUR-09-01503.

REFERENCES

- [1] Ganguly, A. R., et al., *Knowledge Discovery from Sensor Data for Security Applications*, chap 12, 187-204, 2007.
- [2] Parunak, H. Van Dyke, et al., "Swarming Pattern Detection in Sensor and Robot Networks," ANS 10th Conference on Robotics and Remote Systems for Hazardous Environments, 2004.
- [3] Brennan, Sean M., et al., "Radiation Detection with Distributed Sensor Networks," IEEE Computer, Vol. 37, No. 8, Aug. 2004.
- [4] Nemzek, Robert J., "Distributed Sensor Networks for Detection of Mobile Radioactive Sources," IEEE Transactions on Nuclear Science, Vol. 51, No. 4, Aug 2004.
- [5] Stephens, Daniel L., et al., "Detection of Moving Radioactive Sources Using Sensor Networks," IEEE Transactions on Nuclear Science, Vol 51, No. 5, Oct 2004.
- [6] Brennan, Sean M., et al., "Radioactive Source Detection by Sensor Networks," IEEE Transactions on Nuclear Science, Vol. 52, No. 3, Aug 2005.
- [7] Gu, Lin, et al., "Lightweight Detection and Classification for Wireless Sensor Networks in Realistic Environments", SensSys 2005, Nov 2005.
- [8] Viola, Paul A., Jones, Michael J., "Rapid Object Detection using a Boosted Cascade of Simple Features", IEEE Conference on Computer Vision and Pattern Recognition, Vol 1, pp. 511-518, 2001.
- [9] Quinlan, J. Ross, "Induction of decision trees," Machine Learning, pp. 81-106, 1986.
- [10] Frigo, Jan, et al., "Sensor network based vehicle classification and license plate identification system," IEEE INSS 2009.
- [11] Saint Gobain Web Page: http://www.detectors.saint-gobain.com/Media/Documents/S00000000000000001004/SGC_Sodium_Iodide_Data_Sheet.pdf